Tanskanen Eija, I (Orcid ID: 0000-0002-3783-1161)
Snekvik Kristian (Orcid ID: 0000-0003-2650-0057)
Slavin James, A. (Orcid ID: 0000-0002-9206-724X)
Pérez-Suárez David (Orcid ID: 0000-0003-0784-6909)
Goldstein Melvyn, L. (Orcid ID: 0000-0002-5317-988X)
Käpylä Maarit, J (Orcid ID: 0000-0002-9614-2200)
Häkkinen Lasse (Orcid ID: 0000-0003-0755-6661)
Mursula Kalevi (Orcid ID: 0000-0003-4892-5056)

Solar cycle occurrence of Alfvénic fluctuations and related geo-efficiency

E. I. Tanskanen[1], K. Snekvik[2], J.A. Slavin[3], D. Pérez-Suárez[4], A. Viljanen[5], M. L. Goldstein[6], M. J. Käpylä[1,7], R. Hynönen[1], L.V.T. Häkkinen[5], and K. Mursula[8]

[1]Aalto University, ReSoLVE Centre of Excellence, Espoo, Finland (eija.tanskanen@aalto.fi).

[2] Birkeland Centre for Space Sciences, University of Bergen, Norway.

[3] University of Michigan, Ann Arbor, US.

[4] UCL, Mullard Space Sciences Laboratory, UK.

[5] Finnish Meteorological Institute, FI-00100 Helsinki, Finland.

[6] Space Science Institute, Boulder, CO, US

[7] Max Planck Institute for Solar System Research, Göttingen, Germany

[8] Oulu University, Space Climate Research Unit, ReSoLVE Centre of Excellence, Oulu, Finland.

Key point 1: The annual number and duration of Alfvénic solar wind fluctuations (ALFs) varies by an order of magnitude over SC23.

Key point 2: There is an abrupt transition from ALFs being embedded in slow wind until 2002 to ALFs being dominantly in fast wind since 2003.

Key point 3: Substorm frequency increases by 40% from 2002 to 2003, simultaneous to increase of ALF activity.

This is the author manuscript accepted for publication and has undergone full peer review but has not been through the copyediting, typesetting, pagination and proofreading process, which may lead to differences between this version and the Version of Record. Please cite this article as doi: 10.1002/2017JA024385

Abstract

We examine solar wind intervals with Alfvénic fluctuations (ALFs) in 1995 - 2011. The annual number, the total annual duration and the average length of ALFs vary over the solar cycle, having a maximum in 2003 and a minimum in 2009. ALFs are most frequent in the declining phase of solar cycle, when the number of high-speed streams at the Earth´s vicinity is increased. There is a rapid transition after the maximum of solar cycle 23 from ALFs being mainly embedded in slow solar wind (< 400 km/s) until 2002 to ALFs being dominantly in fast solar wind (> 600 km/s) since 2003. Cross helicity increased by 30% from 2002 to 2003, and maximized typically 4-6 hours before solar wind speed maximum. Cross helicity remained elevated for several days for highly Alfvénic non-ICME streams, but only for a few hours for ICMEs. The number of substorms increased by about 40% from 2002 to 2003, and the annual number of substorms closely follows the annual cross helicity. This further emphasizes the role of Alfvénic fluctuations in modulating substorm activity. The predictability of substorm frequency and size would be greatly improved by monitoring solar wind Alfvénic fluctuations in addition to the mean values of the important solar wind parameters.

1. Introduction

The existence of Alfvén waves was predicted in 1942 by Hannes Alfvén [*Alfvén*, 1942]. It is known since then that Alfvén waves occur in the magnetosphere [Cummings et al., 1969] and in the solar wind (SW) [*Coleman*, 1968]. Moreover, a few years ago, Alfvén waves were also observed in the solar corona [*Banerjee et al.*, 2009; *McIntosh et al.*, 2011], where they may have an important role in accelerating the solar wind.

The connection between solar activity and geomagnetic activity was recognized already in 1859 during the famous Carrington storm [*Carrington*, 1859]. The two main forms of geomagnetic activity are geomagnetic storms and substorms [*Birkeland*, 1908; *Chree*, 1912], which are measured by equatorial and high-latitude magnetometers, respectively. The occurrence of storms peaks at solar maximum [*Chapman and Ferraro*, 1930], while the number of substorms peaks a few years later in the declining phase of the solar cycle *[Tanskanen et al., 2002; 2011]*. Substorms occur daily [*Akasofu and Chapman*, 1961; *Kallio et al*., 2000; *Kullen and Karlsson*, 2004] while medium-sized or larger geomagnetic storms occur typically once per month [*Häkkinen et al.*, 2003; *Yakovchouk et al.*, 2012].

The main solar wind drivers of geomagnetic activity are interplanetary coronal mass ejections (ICME) and high-speed streams (HSS) together with co-rotating interaction regions (CIR) [*Sawyer and Haurwitz*, 1976; *Tanskanen et al.*, 2005; *Zhang et al.*, 2007; *Richardson and Cane*, 2012]. However, the relationship of HSSs and ICMEs to geomagnetic activity at different latitudes, as well as their occurrence over the solar cycle, vary considerably [*Holappa et al.*, 2014a; 2014b].

The magnitude and direction of the B_z-component of the interplanetary magnetic field (IMF) is known to be the most important factor controlling energy transfer from the solar wind into the Earth´s magnetosphere [*Fairfield and Cahill*, 1966]. Energy input from the solar wind into the magnetosphere increases as the IMF becomes increasingly antiparallel to the equatorial geomagnetic field (i.e., southward oriented). It is primarily during structures such as large magnetic flux ropes and magnetic clouds of ICMEs when the IMF may attain a long interval of strongly southward orientation [*Burlaga et al.*, 1982], which is required to produce intense storms in the Earth´s magnetosphere [*Holzer and Slavin*, 1981].

Alfvénic waves in the solar wind, on the other hand, can produce repeated periods of weakly negative IMF, typically between -1 and -10 nT. Several papers suggest that Alfvénic waves within the corotating streams enhance substorm activity [*Tsurutani et al.,* 1990; *Tsurutani et al.,* 1995; *D´Amicis et al., 2007*; *McPherron et al.,* 2008], power HILDCAAs (high-intensity long-duration continuous AE activity) [*Tsurutani and Gonzales*, 1987], and contribute to ring current formation [*Søraas et al.,* 2004]. D´Amicis [2011 and 2015] found out that solar wind fluctuations during the maximum phase of solar cycle 23 (SC23) are highly Alfvénic. Roberts and Goldstein [1990] reported that Alfvénic intervals often accompany large and extended auroral activity, although the reverse was not found to be true. They examined intervals around the maximum of solar cycle when the interplanetary Alfvén waves and their effects to geomagnetic activity are more often due to the slow solar wind [*Gonzalez et al.*, 1995; *Chian et al.,* 2006; *D´Amicis et al.*, 2007].

In this paper, we study solar wind Alfvénic fluctuations (ALFs), in particular their occurrence in 1995-2011 and relation to high-latitude geomagnetic activity. Earlier studies on the same topic had more limited time range, and did not cover a full solar cycle. We calculate the annual number and total duration of ALFs, as well as their mean cross helicity. We study how cross helicity is distributed in time for ALFs within ICME-related solar wind, and highly and weakly Alfvénic not-ICME-related solar wind. We also calculate the annual occurrence of ALFs within fast and slow solar wind separately, and examine how the number of substorms and storms vary during the time interval 1995-2011.

2. Data and methods

We have developed data mining tools to find Alfvénic fluctuations and high-speed streams (with a code called HSSeeker), and to determine storm and substorm occurrence rates (SSeeker; *Tanskanen et al.,* 2005) in order to compare the different solar wind structures (ICME, HSS, slow wind) and ALFs related to these structures with different forms of space weather in the Earth´s magnetosphere. The initial search for solar wind streams was done using the 5-minute data of the OMNI-2 database [*King and Papitashvili*, 2005], as explained in Snekvik et al. [2013]. However, the helicity analysis was done using original measurements by the WIND and ACE spacecraft in order to preserve the spectral properties of the IMF, which may be modified in the OMNI data due to the shift of the data from the site of observation to the bow shock of the Earth's magnetosphere. For the WIND spacecraft, we used the 92 s data of the SWE plasma instrument [*Ogilvie et al., 1995*], and the 3 s version-5

magnetic field data of the MFI instrument [Lepping et al., 1995]. For the ACE satellite, we used the 64 s Level-2 proton data of SWEPAM instrument [*McComas et al., 1998*], and the 16 s Level-2 magnetic field data of MAG instrument [*Smith et al., 1998*]. The higher-sampling magnetic data were median averaged to the lower sampling frequency of the plasma data of the respective satellite. We used WIND and ACE data alternatingly, selecting the data of that satellite which had a more complete dataset (less data gaps) available for any 512-point averaging interval. Note also that, because of the long 512-point averaging interval, no practical difference in results was found between the slightly differently sampled WIND and ACE data.

The cross helicity

$$H_c = \langle \mathrm{v}' \cdot \mathrm{v}'_A \rangle \tag{1}$$

is a measure of the correlation between the fluctuations of solar wind velocity and Alfvén velocity (v´and v_A´, respectively). (The mean is denoted by < > and taken here over a sample interval of 512 data points). Solar wind ALFs are identified by the normalized cross helicity [*Tu and Marsch*, 1995; *Snekvik et al.*, 2013]

$$\sigma_c = \frac{2\langle \mathrm{v}' \cdot \mathrm{v}'_A \rangle}{\langle \mathrm{v}'^2 \rangle + \langle \mathrm{v}'^2_A \rangle} = \frac{Var(Z_{out}) - Var(Z_{in})}{Var(Z_{out}) + Var(Z_{in})} \tag{2}$$

where Var means the variance of Z_{out} = v´- v_A´ and Z_{in} = v´+ v_A´, the two Elsässer variables denoting the outward and inward propagating Alfvén waves for an outward oriented IMF, respectively (for more information, see *Tu and Marsch*, 1995; *Snekvik et al.*, 2013). For inward IMF the signs are interchanged, i.e., Z_{out} = v´+ v_A´ and Z_{in} = v´- v_A´. In solar wind at 1AU, the outward propagating Alfvén waves are much more common than inward propagating waves. Accordingly, the typical values of σ_c are positive, even fairly close to one, rather than negative [*Snekvik et al.*, 2013]. Alfvénic intervals are generally identified and classified based on the value of the normalized cross helicity.

We have calculated the cross helicity H_c and the normalized cross helicity σ_c for each 512-point sample interval of about 9 hours for ACE data and 13 hours for WIND data, stepping at 2-hour steps. (The magnetic field direction is rather uncertain close to the IMF field reversal. Therefore, we have removed all measurements within 12 hours of IMF reversal from the analysis). The sample interval is here defined to be Alfvénic if

the normalized cross helicity equals or exceeds 0.8. An ALF interval is typically longer than one sample interval, beginning when the normalized cross helicity exceeds 0.8 and ends when it decreases below 0.8.

We use here ground-based magnetic field measurements from the high-latitude IMAGE network [*Tanskanen*, 2009] in Fenno-Scandinavia in 1995 - 2011. We identify substorms from the westward electrojet index, IL index, [*Kallio et al*, 2000] constructed from IMAGE data. Figure 1 depicts the IL index (in nT) in 1995 - 2011 at monthly resolution (for separate UT hours), color-coded so that blue shows the smallest activity and yellow the largest activity. Only the time interval between 18 - 04 UT is shown, when the IL magnetometers are located around the midnight, where substorms occur. Figure 1 shows that the largest high-latitude geomagnetic activity is observed during the early declining phase of SC23 with a rapid increase in late 2002 and a decrease after 2003. Geomagnetic storms are identified from the geomagnetic Dst index [*Sugiura*, 1964]. A storm is in progress when the Dst is below -50 nT.

3. Annual number and duration of ALFs

Figure 2 shows the ALF occurrence rate, i.e., the annual ALF numbers in 1995 - 2011, covering the whole solar cycle 23. ALFs are observed in each year, but there is a large variation over the solar cycle. There is a high ALF number period of more than 60 ALFs per year from 1999 to 2005, with a maximum ALF number in 2003, when more than 100 ALFs are observed (roughly 8 per solar rotation). The smallest number of ALFs is found at sunspot minimum in 2009, when only 10 ALFs occurred in the entire year. Accordingly, the number of ALFs varies roughly by one order of magnitude during SC23.

Figure 2 also depicts the total annual duration of ALF intervals in days. In 2003 the ALF activity covered 189 days, i.e., more than half a year. Taking into account the fact that there are some gaps in the data (as discussed above), this is an impressive coverage. Annual ALF duration was roughly three times longer for ALF active years (ALF number > 60) than for less active years (ALF number < 60). In 2009 the total ALF activity covered only 7 days. Comparing to the year 2003, this implies that the solar cycle variation in annual ALF duration was even relatively larger than in ALF occurrence. This also suggests that there is a solar cycle variation in the (annually

averaged) mean length of ALFs so that a typical ALF is somewhat longer in the ALF active years than in less active years.

Next we divided the ALFs into two categories: slow solar wind (SW) ALFs if the mean speed during the ALF is at most 400 km/s and fast solar wind ALFs if the solar wind speed during the ALF equals or exceeds 600 km/s. Figure 3 shows the annual number of fast and slow solar wind ALFs separately. The occurrence rate of slow solar wind ALFs increases fairly systematically from the previous solar minimum to a maximum in 2002, but then declines rapidly in 2003. On the other hand, the number of fast SW ALFs remains rather small until 2002, clearly below the number of slow SW ALFs, but then rapidly increases to a maximum in 2003. The number of fast SW ALFs remains quite high until 2008, far higher than the number of slow SW ALFs.

These results show a rapid transition in the properties of solar wind speed carrying ALFs when turning from the solar cycle maximum to the declining phase of the SC23. Figure 3 also includes the annual means of solar wind speed, showing that the annual solar wind speed increased from 440 km/s in 2002 to 540 km/s in 2003. It is known that HSSs dominated most of the year 2003 [*Tanskanen et al., 2005; Mursula et al.*, 2015] and the solar wind speed was exceptionally high especially during the solstice months [*Mursula et al.*, 2017]. Accordingly, the rapid increase of the mean solar wind speed from 2002 to 2003 is manifested as a rapid decline of ALFs carried by the slow solar wind and an increase of ALFs carried by the fast solar wind.

4. Annual cross helicity of ALFs

Figure 4a shows the yearly averaged cross helicity of all ALFs of the year. Note that for the cross helicity to attain a large value, both the ALF amplitude (denominator of Eq. 2) and alignment (normalized cross helicity, Eq. 1) have to be large. Yearly averaged cross helicity varies from the minimum of less than 500 km^2/s^2 in 1997 (solar minimum year between SC22 and SC23) to the maximum of about 2000 km^2/s^2 in 2003. During the minimum between SC23 and SC24 cross helicity reached another deep local minimum, at a slightly higher level than during the previous minimum. Note that the mean cross helicity in 2000, during the maximum of SC23, is only 30% larger than during the next solar minimum, and reaches only 60% of the maximum value in 2003. The yearly mean values exceeding 1400 km^2/s^2 (dotted horizontal line in Fig. 4a) are only seen during the declining phase in 2002 - 2003 and 2005 - 2008.

The yearly averaged solar wind speed during ALFs is depicted in Figure 4b. One can see that the yearly mean ALF solar wind speed increases from 2002 to 2003 by almost the same percentage as the full annual means of solar wind speed (see Fig. 3), but the ALF speeds are slightly higher than the mean speeds, due to the selection effect of ALFs. However, the ALF solar wind speed attains only a local maximum in 2003, and somewhat higher values of up to 600 km/s are found during the late declining phase in 2005 - 2008, with a maximum in 2008. This seemingly surprising result is due to the fact that, as Figures 2 and 3 show, there are some 50 (about 65%) intermediate-speed ALFs (400 km/s < v < 600 km/s) in 2003 but only some 15 (45%) in 2006-2008. Moreover, the relative fraction of slow wind ALFs is decreasing from 2005 to a minimum in 2008, leading to a maximum in Fig. 4b in 2008.

Both panels of Fig. 4 show the annual numbers of substorms, which follow fairly reliably the evolution of the mean annual cross helicity (Fig. 4a). Accordingly, the correlation between the substorm number and cross helicity is very good (Pearson correlation coefficient r = 0.7, probability of random correlation p = 0.004). On the other hand, correlation between the substorm number and mean ALF speed remains insignificant (r = 0.3, p = 0.22) because of the above discussed maximum in the late declining phase of SC23 in ALF mean speed.

The annual number of those ALFs whose cross helicity H_c is larger than 1000 km^2/s^2 is shown in Figure 5. These form the part of ALFs (for which $\sigma_c \geq 0.8$) where the amplitude of the fluctuations of the solar wind velocity and magnetic field is largest. Figure 5 shows a roughly similar solar cycle variation as depicted by the mean ALF cross helicity in Fig. 4a. However, the maximum in 2003 is further emphasized, especially with respect to the situation in the later declining phase of the cycle. In 2003 more than 80% of ALFs have a cross helicity larger than 1000 km^2/s^2. On the other hand, in 2009 the large-cross helicity ALFs practically vanish. Thus, the solar cycle variation of large-cross helicity ALFs is relatively even larger than for ALF number or duration.

5. ALFs embedded within different solar wind structures

Alfvénic fluctuations can appear in both slow and fast speed streams as well as ICMEs [*Roberts et al.*, 1987; *Snekvik, 2013*]. We used here the division of solar wind

to these three solar wind structures (partly also unspecified solar wind), based on 5-minute OMNI data, median filtered over 10 hours (for more details, see Snekvik et al., 2013). We calculated the cross helicities and normalized cross helicities for ICMEs and non-ICME structures. The latter were further divided into two classes: the highly Alfvénic streams (high-ALFs) and weakly Alfvénic streams (weak-ALFs) according to the mean value of $\sigma_c \geq 0.8$ or $\sigma_c < 0.8$ during the stream, respectively. The highly Alfvénic streams are a part of ALFs discussed above, but the weakly Alfvénic streams are a new class outside the ALF definition adopted above. Note that although a considerable amount of ICMEs are included within ALFs (as defined and studied above), there are also several ICMEs that are not ALFs (i.e., do not have $\sigma_c > 0.8$).

We have made a superposed epoch (SPE) analysis [*Brier and Bradley*, 1964] for the cross helicity H_c separately for ICMEs and non-ICMEs (high-ALF and weak-ALF). The SPE-curve was computed from three days before to three days after the maximum speed of the stream, which was selected as the superposed zero time (t = 0). Figure 6 depicts the superposed values of the cross helicity for high-ALF streams (red curve), ICMEs (green curve) and weak-ALF streams (black curve). Interestingly, the cross helicity is found to maximize several (typically 4-6) hours before the velocity maximum for all three solar wind structures. This means that the time evolution of cross helicity within the compression region before the solar wind speed maximum is quite similar for high-ALF, weak-ALF and ICME-related structures.

The peak magnitude of SPE cross helicity for weakly Alfvénic streams (358 km^2/s^2) is, as expected, much lower than the corresponding peak for the highly Alfvénic streams (929 km^2/s^2). More interestingly, the peak SPE cross helicity of ICMEs (521 km^2/s^2) is only 56% of the peak of the highly Alfvénic streams, but still notably higher than for weak-ALF streams. The cross helicity SPE curve for ICMEs is also more limited around zero time than for either of the two other ALF groups. The interval of elevated SPE cross helicity lasts for several days for high-ALFs, but only for a few hours for ICMEs and weak-ALF streams. The average cross helicity over the whole 6-day SPE interval for ICMEs is 203 km^2/s^2, for high-ALFs 450 km^2/s^2 and for low-ALFs 140 km^2/s^2. Thus, the average cross helicity for ICMEs is less than half of the average cross helicity for high-ALFs and only somewhat larger than for weak-ALFs.

The distribution of solar wind speed during the three structures is shown in Figure 7. One can see that about 50% of highly Alfvénic streams have a speed of ≥600 km/s and could be classified among high-speed streams. On the other hand, only 18% of weakly Alfvénic streams belong to HSS category. Instead, about 44% of weakly

Alfvénic streams have a slow speed of ≤450 km/s. Therefore, one can roughly equate the highly Alfvénic streams as high-speed streams and the weakly Alfvénic streams as slow-speed streams. The solar wind speed during ICMEs varies more than during the two other streams. About 35% of ICMEs belong to the high-speed category, while 30% have a slow speed of ≤450 km/s. The mean speed of ICMEs is as high as 582 km/s, due to the long tail of the speed distribution (see Fig. 7).

These results show that high-speed streams, which also cause most of substorms and high-latitude activity [*Tanskanen et al.*, 2005; *Holappa et al.*, 2014a], include typically somewhat larger cross helicities than ICMEs, which are mainly responsible for intense magnetic storms and low-latitude geomagnetic activity.

6. Annual numbers of ICMEs, HSSs, storms and substorms

We examine now the annual occurrence rate of substorms and storms, and their two most important solar wind drivers, the ICMEs and HSS/CIRs over the solar cycle 23. Figure 8 depicts the annual numbers of substorms (R_{ss}), storms (R_{st}), HSSs and ICMEs in 1997-2010. (Yearly sunspot numbers, denoted by grey shaded areas, are included in each panel for reference). Storm numbers R_{st} are depicted in Figures 8b, 8d and 8f, and the largest number of storms is found in 2003. The storm numbers of more than 20 storms in a year are found in 1997, 2000 - 2003, and in 2005.

Annual substorm numbers are depicted in Figures 8a, 8c and 8e. (Note that substorm numbers used here are based on IMAGE magnetometers, which can reliably detect substorms in the 16-02 UT (18-04 LT) sector, when the IMAGE magnetometers are located at the nightside). Substorms occur at a fairly similar frequency of about 450-500/year in the ascending phase over the solar maximum until 2002, and again in the later declining phase from 2006 to 2008. The highest frequency of substorms is detected in 2003 - 2005, when the substorm number exceeded 600/year. Year 2003 marks the maximum of substorm occurrence with 699 substorms, while in 2009 substorm occurrence was clearly lower than in any other year of SC23. Note that although year 2003 marked the maximum occurrence of both storms and substorms, the distribution of storms and substorms over the solar cycle 23 was clearly different. A large majority of storms occurred before 2003 but most substorms only thereafter.

The highest annual occurrence rates of ICMEs [*Cane and Richardson*, 2003; *Richardson and Cane*, 2012; *Kilpua* et al., 2012] (green curve in Figs. 8c and 8d) are observed during the sunspot maximum in 2000-2001. Yearly ICME numbers correlate very well with the sunspot numbers (correlation coefficient r = 0.8, p = 0.0002, not shown in Fig. 8), in agreement with the fact that ICMEs are related to magnetic structures like prominences originating from active regions of the Sun. The correlation between storm numbers and ICME numbers is also highly significant (r = 0.7, p = 0.004), but the correlation between the substorm numbers and ICMEs is insignificant (r = 0.2, p = 0.5). On the other hand, the number of substorms and high-speed streams (red curve in Figs. 8e and 8f) correlates very well (r = 0.8, p = 0.0004), supporting the earlier result that substorms are mainly driven by high-speed streams [*Tanskanen et al.*, 2005; *Richardson and Cane*, 2012]. However, storm numbers and high-speed streams do not vary similarly over the solar cycle (r = 0.2, p = 0.5).

7. Discussion

Interplanetary Alfvén waves with magnetic field fluctuations including periods of southward IMF are known to be important in increasing the dayside reconnection rate and enhancing geomagnetic activity especially at high latitudes [*Tsurutani and Gonzalez*, 1987; *Tsurutani et al.*, 1990; *Hsu and McPherron*, 2002; *D´Amicis et al.*, 2006, 2007, 2011]. The importance of the IMF southward component for geomagnetic activity was discovered as early as mid-1960´s [*Fairfield and Cahill*, 1966]. *Tsurutani et al.* [1990] examined the connection between Alfvén waves and substorm activity in 1979, and *Lee* et al. [2006] the effect of northward turnings of IMF B_z during Alfvénic intervals in 1996-2002.

Tsurutani and Gonzalez [1987] found that large-amplitude Alfvén waves occurred in the trailing portions of high-speed solar wind streams, and that Alfvén waves were present during HILDCAA events. *D´Amicis et al.* [2007] reported that Alfvénic fluctuations were particularly geoeffective in 1995 (in the late declining phase of SC22) while they were less geoeffective during solar maximum. Previous studies on Alfvénic fluctuations have concentrated on examining rather short time intervals or earlier times [*Tsurutani et al.*, 1995*; D´Amicis et al., 2007*].

In this paper we have examined the properties of Alfvénic fluctuations and their relation to geomagnetic activity in 1995 - 2011, covering well the full solar cycle 23. We have determined the yearly numbers and durations of Alfvénic fluctuations (see

Fig. 2) and the ALF-related solar wind speed (see Fig. 4b) over the solar cycle, as well as the annual numbers of substorms and storms (see Fig. 8). Alfvénic fluctuations are found throughout the solar cycle [*Snekvik et al.*, 2013], but they clearly maximize in the year 2003, during the declining phase of SC23.

We found a rapid increase in yearly averaged ALF cross helicity during the early declining phase of the SC23, when the yearly averaged cross helicity increased by roughly 30% from 2002 to 2003 (see Fig. 4a). Even thereafter, the ALF cross helicity was enhanced practically during the entire declining phase of SC23 until (and including) 2008. The change from 2002 to 2003 was examined in more detail by dividing the ALFs based on the related solar wind speed. The slow solar wind ALFs (speed < 400 km/s) dominated during the ascending phase and solar maximum of SC23 until 2002, while the fast ALFs (speed ≥ 600 km/s) started dominating abruptly in 2003 and dominated the declining phase of both SC23 and SC22. This rapid change from 2002 to 2003 is suggested to be due to the simultaneous increase in the mean solar wind, as more and more of HSSs started appearing at this time due to the development of both polar and low-latitude coronal holes [*Mursula et al.*, 2015; 2017]. The sharp increase in fast solar wind ALFs coincided with the increase of substorm intensity and number.

We have also studied here the Alfvénic properties of three different solar wind structures: ICMEs, as well as highly Alfvénic ($\sigma_c \geq 0.8$) and weakly Alfvénic ($\sigma_c < 0.8$) non-ICME streams. We showed that the highly Alfvénic (non-ICME) streams typically have a fairly high solar wind speed, and a large fraction could be classified as HSSs with speed faster than 600 km/s. On the other hand, the weakly Alfvénic streams typically have clearly slower speeds, although a fraction of HSSs are also rather weakly Alfvénic (i.e., have a small σ_c). Interestingly, the ICMEs have a very wide and flat distribution of solar wind speeds, including roughly one third of typically HSS speeds with a very long tail of speeds above 600 km/s, and one third of slow speeds below 450 km/s.

The distribution of cross helicity within the three solar wind structures was studied using the superposed epoch analysis. The SPE peak cross helicity for the highly Alfvénic streams was found to be about 930 km^2/s^2, while for ICMEs it was about 520 km^2/s^2. For average SPE cross helicities the relative difference between high-ALF streams and ICMEs was even larger (450 km^2/s^2 and 203 km^2/s^2, respectively). These results agree with the earlier observations reported by *Belcher and Davis* [1971], who showed, based on Mariner 5 data in 1967, that the most Alfvénic solar wind is observed during the high-speed streams.

We also found that cross helicity stays enhanced for several days after the peak for highly Alfvénic streams, but drops sharply only few hours after the peak for ICMEs. This indicates that the HSS-related solar wind includes a considerably larger total amount of Alfvénicity than ICME-related solar wind. These results suggest that the role of Alfvénic fluctuations in modulating substorm activity is larger during HSSs than during ICME-related solar wind. The predictability of substorm frequency and size may be improved by monitoring the solar wind Alfvénic fluctuations in addition to the mean values of solar wind speed and magnetic field.

8. Main results and conclusions

We have shown that the characteristics of Alfvénic fluctuations in solar wind abruptly changed when the solar maximum of cycle 23 turned into the declining phase. While until 2002 the Alfvénic ($\sigma_c \geq 0.8$) intervals were mainly found in slow solar wind, from 2003 onwards they were dominantly found in high-speed streams. The yearly averaged cross helicity increased by 30% from 2002 to 2003. These abrupt changes are related to the increase of the yearly averaged solar wind speed from about 440 km/s in 2002 to 540 km/s in 2003 and, in particular, to the increasing number of high-speed streams within the solar wind.

Overall, the number of Alfvénic intervals varies roughly by one order of magnitude during SC23 from maximum of about 100 in 2003 to a minimum of 10 per year in 2009. The total annual duration of ALFs varies from more than 50% of time in 2003 to only 7 days in 2009. The solar cycle variation is relatively larger in ALF duration than in ALF occurrence, implying a solar cycle variation also in the average ALF length. ALFs are typically somewhat longer in the ALF active years than in less active years. Solar cycle variation is even larger in those ALFs that have higher than average cross helicity.

Cross helicity maximizes typically 4-6 hours before the solar wind speed maximum, irrespective of solar wind structure. For ICMEs the peak superposed cross helicity was roughly half of high-ALF streams and only somewhat higher than for weakly Alfvénic streams. Moreover, the interval of elevated cross helicity lasts for several days for highly Alfvénic streams, but only for a few hours for ICMEs, leading to a

considerably larger total amount of cross helicity in HSS related streams than in ICME-related solar wind.

The change in solar wind structure and the increase in the amount of Alfvénic fluctuations in 2003 coincide with the increase of substorm frequency by about 40%. Periodic southward intervals typical of highly Alfvénic solar wind produce repeated substorm intervals. Year 2003 marks the maximum occurrence of both storms and substorms, but the distribution of storms and substorms over the solar cycle is clearly different. A large majority of storms occurred before 2003 but most substorms thereafter. The annual number of substorms follows fairly reliably the evolution of the mean annual cross helicity. Our results suggest that the role of Alfvénic fluctuations in modulating substorm activity is large. Accordingly, the predictability of substorm frequency and size would be greatly improved by monitoring the solar wind Alfvénic fluctuations in addition to the average values of the important solar wind parameters such as magnetic field and speed.

References

Akasofu, S.-I. and Chapman, S. (1961), The ring current , geomagnetic disturbance, and Van Allen radiation belts, *Planet Space Sci.* 66, 1321.

Alfvén, H. (1942), Existence of Electromagnetic-Hydromagnetic Waves, *Nature*, 150, 405.

Banerjee, D., D. Pérez-Suárez, and J.G. Doyle (2009), Signatures of Alfvén Waves in the polar coronal holes as seen by EIS/HINODE, *Astron.&Astrophys.*, 501, L15-L18.

Belcher, J. W. and J. Davis Jr. (1971), Large-Amplitude Alfvén waves in the Interplanetary Medium, 2, *J. Geophys. Res*, 76, 3534.

Birkeland, K. (1908), *The Norwegian Aurora Polaris Expedition 1902-1903* [vol 1, 1st sect.] Aschhoug, Oslo, Norway.

Brier, G. W. and D.A. Bradley (1964), The lunar synodical period and precipitation in the United States, *J. Atmos. Sci.* 21, 386-395.

Burlaga, L. F. et al. (1982), A magnetic cloud and a coronal mass ejection, *Geophys. Res. Lett.* 12, 1317.

Cane, H. V. and I.G. Richardson (2003), Interplanetary coronal mass ejections in the near-Earth solar wind during 1996-2002, *J. Geophys. Res.* 108 (A4).

Carrington, R. (1859), Description of a Singular Appearance seen in the Sun on September 1, 1859, *Monthly Notices of the Royal Astronomical Society*, 20, 13-5.

Chapman, S. and V. C. A. Ferraro (1930), A new theory of magnetic storms, *Nature*, **129**, 3169.

Chree, C. (1912), *Studies in Terrestrial magnetism*, 206, McMillan and Co., London and New York.

Chian, A.C.-L., Y. Kamide, E. L. Rempel, and W. M. Santana (2006), On the chaotic nature of solar-terrestrial environment: Interplanetary Alfvén intermittency, *J. Geophys. Res*., 111, A07S03, doi:10.1029/2005JA011396.

Coleman, P. J., Jr. (1968), Turbulence, viscosity, and dissipation in the solar-wind plasma, *Astrophys.J.*, 153, 371.

Cummings, W. D., R. J. O´Sullivan, P. J. Coleman Jr. (1969), Standing Alfvén waves in the magnetosphere, *J. Geophys. Res*., 74, 778.

D´Amicis, R., R. Bruno, B. Bavassano, V. Carbone, L. Sorriso-Valvo (2006), On the scaling of waiting-time distributions of the negative IMF Bz component, *Ann. Geophys.*, 24, 10, 2735.

D´Amicis, R., R. Bruno and B. Bavassano (2007), Is geomagnetic activity driven by solar wind turbulence, *Geophys. Res. Lett.*, 34, doi:10.1029/2006GL028896.

D´Amicis, E., R., Bruno, and B. Bavassaro (2011), Response of the geomagnetic activity to solar wind turbulence during solar cycle 23, *J. Atmos. Sol.-Terr. Phys.*, 83(5-6), 653, doi:10.1016/jastp.2011.01.012.

D´Amicis, E., and R. Bruno (2015), On the origin of highly Alfvénic slow solar wind, *Astrophys. J.*, 805:84.

Fairfield, D. H., and L. J. Jr. Cahill (1966), Transition region magnetic field and polar magnetic disturbances, *J. Geophys. Res*., 71, 155.

Gonzalez, W. D., A.L. Clúa de Gonzalez, and B.T. Tsurutani (1995), Geomagnetic response to large-amplitude interplanetary Alfvén wave trains, *Phys. Scr*. 55, 140-143.

Holappa, L. et al. (2014a), Annual fraction of high-speed streams from principal component analysis of local geomagnetic activity, *J. Geophys. Res.*, 119, 4544.

Holappa, L., et al. (2014b), A new method to estimate annual solar wind parameters and contributions of different solar wind structures to geomagnetic activity, *J. Geophys. Res.*, 119, 9407.

Holzer, R. E. and J. A. Slavin (1981), The effect of solar wind structure on magnetospheric energy supply during solar cycle 20, *J. Geophys. Res.*, 86, 675.

Hsu, T.-S., and R. L. McPherron (2002), An evaluation of the statistical significance of the association between northward turnings of the interplanetary magnetic field and substorm expansion onsets, *J. Geophys. Res.*, 107(A11), 1398, doi:10.1029/2000JA000125.

Häkkinen, L. V. T., et al. (2003), Seasonal and diurnal variation of geomagnetic activity: revised Dst versus external drivers, *J. Geophys. Res.*, 108(A2).

Kallio , E.I., et al. (2000), Loading-unloading processes in the nightside ionosphere, *Geophys. Res. Lett.* 27, 1627.

Kilpua, K.E.J., Jian, L.K., Li, Y., Luhmann, J.G. and Russell, C.T. (2012), Observations of ICMEs and ICME-like solar wind structures from 2007-2010 using near-Earth and STEREO observations, Solar Physics, 281, 391.

Kullen, A., and Karlsson, T. (2004), On the relation between solar wind, pseudobreakups and substorms, *J. Geophys. Res.* 109(A12).

Lee, D.-Y, L.R. Lyons, K.C. Kim, et al. (2006), Repetitive substorms caused by Alfvénic waves of the interplanetary magnetic field during high-speed solar wind streams, *J. Geophys. Res.*, 111(A12), CiteID A12214.

Lepping, R., et al. (1995), The wind magnetic field investigation, *Space Sci.*

Rev., 71, 207–229, doi:10.1007/BF00751330.

McIntosh, S. W., B. De Pontieu, M. Carlsson, V. Hansteen, P. Boerner, M. Goossens (2011), Alfvénic waves with sufficient energy to power the quiet solar corona and fast solar wind, *Nature*, 475, 7357, DOI:10.1038/nature10235.

McPherron, Robert L., James M. Weygand, and Tung-Shin Hsu (2008), Response of the Earth's magnetosphere to changes in the solar wind, *J. Atmos. and Sol-Terr. Phys.* 70.2, 303-315.

Mursula, K., R. Lukianova, and L. Holappa (2015), Occurrence of high-speed solar wind streams over the Grand Modern Maximum, *Astrophys. J.* 801, 30, http://dx.doi.org/10.1088/0004-637X/801/1/30.

Mursula, K., L. Holappa, R. Lukianova (2017), Seasonal solar wind speeds for the last 100 years: Unique coronal hole structure during the peak and demise of the Grand Modern Maximum, *Geophys. Res. Lett.* 44, 1, 30-36.

Richardson, I. G., and Cane H. V. (2012), Solar wind drivers of geomagnetic storms during more than four solar cycles, J. Space Weather Space Clim., 2(A01), DOI: 10.1051/swsc/2012001.

Roberts, D. A., Goldstein, M.L., Klein, L.W., and Matthaeus, W.H. (1987), The nature and evolution of magnetohydrodynamic fluctuations in the solar wind: Voyager observations *J. Geophys. Res.* 92, 12 023-12 035.

Roberts, D. A., and M. Goldstein (1990), Do interplanetary Alfvén waves cause auroral activity?, *J. Geophys. Res.* 95(A4), 4327-4331.

Sawyer, C., and M. Haurwitz, J. Geophys. Res. (1976), Geomagnetic activity at the passage of high-speed streams in the solar wind, *J. Geophys. Res.*, 81, 13.

Snekvik, K., Tanskanen, E.I. and Kilpua, K.E.J. (2013). An automated identification method for Alfvenic streams and their geoeffectiveness, *J. Geophys. Res.* 118, 1-13.

Sugiura, M. (1964), Hourly values of equatorial Dst for the IGY, *Ann. Int. Geophys. Year*, 35, 49.

Søraas, F., et al. (2004), Evidence for particle injection as the cause of Dst reduction during HILDCAA events, *J. Atmos. Sol.-Terr. Phys.*, 66, 2, 177.

Tanskanen, E.I. et al. (2002), Substorm energy budget during low and high solar activity: 1997 and 1999 compare (2002), *J. Geophys. Res.*, 107(A6).

Tanskanen, E.I., et al. (2005), Magnetospheric substorms are strongly modulated by interplanetary high-speed streams, *Geophys. Res. Lett.* 32, L16104.

Tanskanen, E.I. (2009), A comprehensive high-throughput analysis of substorms observed by IMAGE magnetometer network: Years 1993-2003 examined, *J. Geophys. Res.* 114(A5).

Tanskanen, E.I. et al. (2011), From space weather toward space climate time scales: Substorm analysis from 1993 to 2008, *J. Geophys. Res.*, 116, A00143.

Tsurutani, B. T., and W. D. Gonzalez (1987), The cause of high-intensity long-duration continuous AE activity (HILDCAAs): interplanetary Alfven wave trains, *Planet. Space Sci.*, 35 (4), 405-412.

Tsurutani, B. T., T. Gould, B. E. Goldstein, W. D. Gonzalez, and M. Sugiura (1990), Interplanetary Alfvén waves and auroral (substorm) activity: IMP 8, *J. Geophys. Res.*, 95, 2241.

Tsurutani, B., et al., (1995), Interplanetary origin of geomagnetic activity in declining phase of the solar cycles, *J. Geophys. Res.*, 100(A11), 21717.

Tu, C. Y., and E. Marsch (1995), MHD structures, waves and turbulence in the solar wind: Observations and theories, *Space Sci. Rev.*, 73, 1-210, doi:10.1007/BF00748891.

Yakovchouk, O. S., Mursula, K., Holappa, L., Veselovsky, I.S., and Karinen, A. (2012), Average properties of geomagnetic storms in 1932-2009, *J. Geophys. Res.*, 117(A3).

Zhang, J., et al. (2007), Solar and interplanetary sources of major geomagnetic storms (Dst $\leq$ 100 nT) during 1996 – 2005, *J. Geophys. Res.*, 112, A10102, doi:10.1029/2007JA012321.

Acknowledgments

We wish to thank the institutes maintaining the IMAGE magnetometer network. The IMAGE magnetic field measurements are available via http://space.fmi.fi/image/beta/ and auroral substorm and storm lists via http://www.substormzoo.org. The sunspot data were archived through SIDC-team, World Data Center for the Sunspot Index, Royal Observatory of Belgium, and interplanetary measurements via CDAWeb archive. The ICMEs are taken from the http://www.srl.caltech.edu/ACE/ASC/DATA/level3/icmetable2.htm, which is a catalogue by Richardson and Cane, and from the ACE ICME catalogue at http://www.srl.caltech.edu/ACE/ASC/. We acknowledge the financial support by the Academy of Finland to the ReSoLVE Centre of Excellence (project no. 272157), and by the European Community´s Seventh Framework Program under grants no. 313038/STORM and no. 283676/ESPAS. M.K. acknowledges funding from the "Active Suns" research project of Helsinki University. We thank D.A Roberts and A.J. Tanskanen for inspiring and constructive comments.

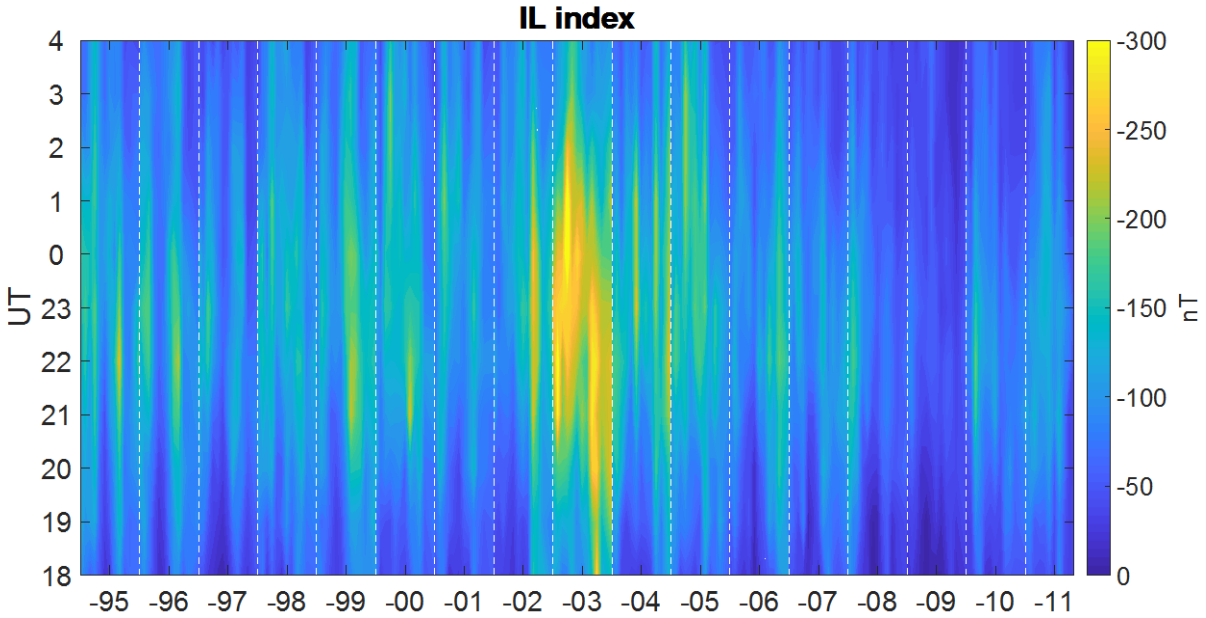

Figure 1. High-latitude geomagnetic activity based on IL, the westward electrojet index in Scandinavian sector in 1995 - 2011. Amplitude of IL index (in nT) is color-coded such that the largest monthly disturbances are shown by yellow and smallest by blue.

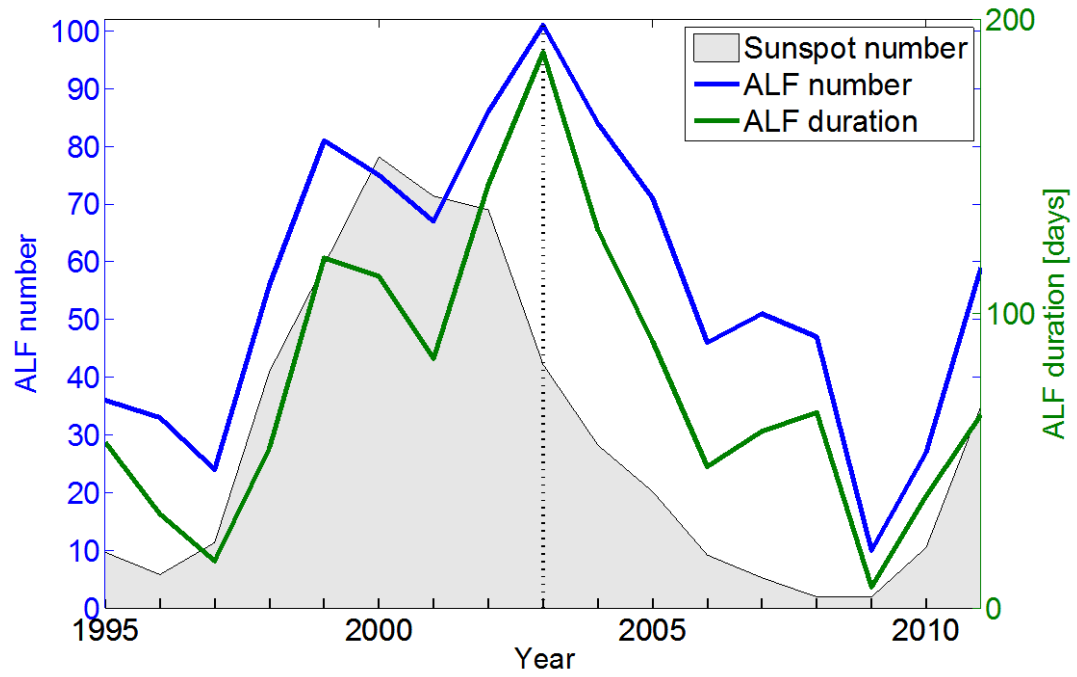

Figure 2. Yearly number of Alfvénic fluctuations in 1995 - 2011 (blue line) and yearly total ALF duration in days (green line; right y-axis). Sunspot numbers are shown as a gray shaded area for reference. Year 2003 is marked by a dotted vertical line.

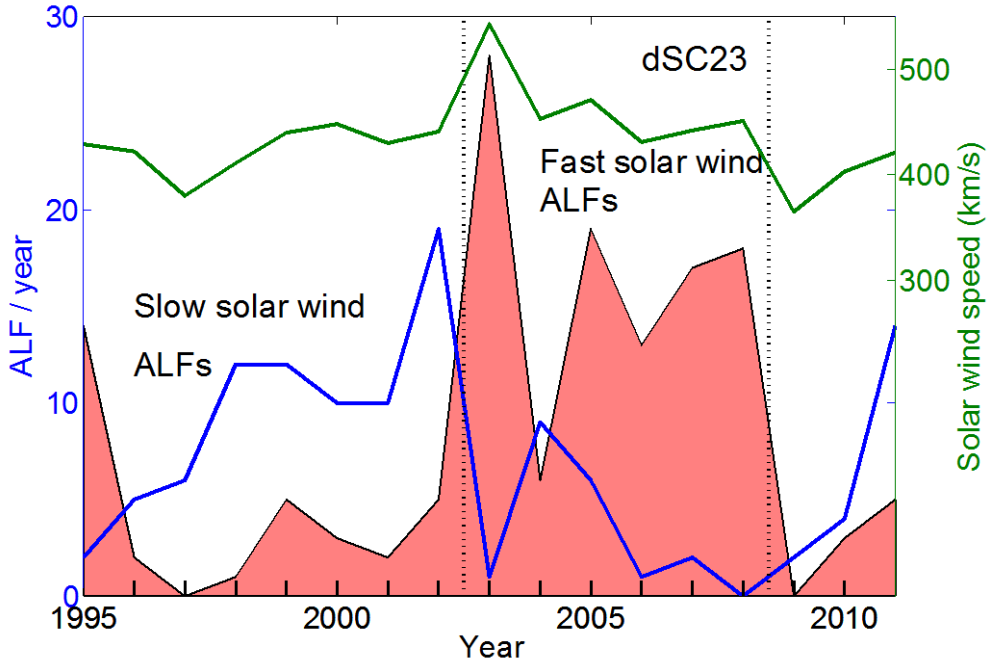

Figure 3. Yearly number of ALFs (left y-axis) within slow (< 400 km/s) solar wind (blue line) and within fast (≥ 600 km/s) solar wind (black line with pink shaded area) in 1995 – 2011. Yearly means of solar wind speed (right y-axis) are denoted by a green line. Declining phase of SC23, dSC23, is marked by dotted vertical lines.

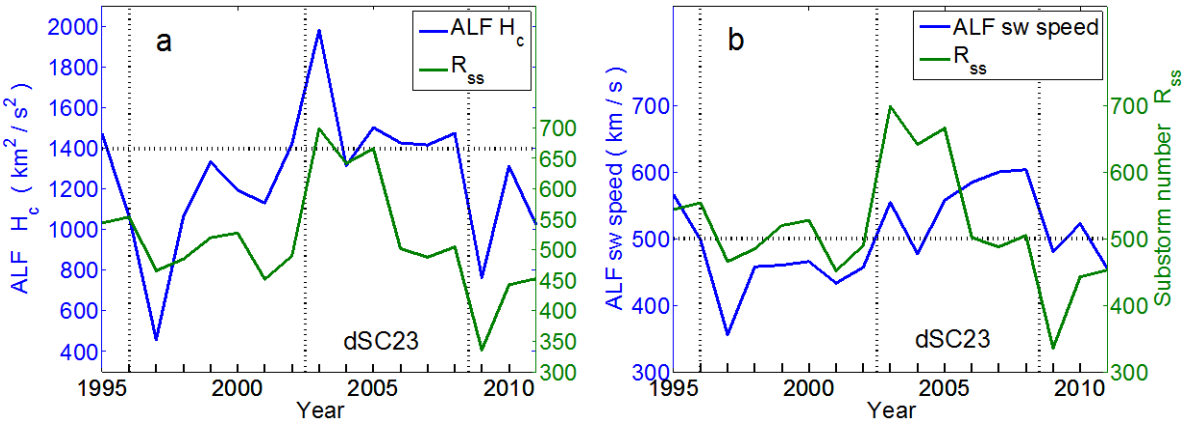

Figure 4. Yearly averaged a) cross helicity of ALFs (blue curve, left y-axis) and b) solar wind speed during ALF intervals (blue curve, left y-axis) in 1995 - 2011. Yearly averaged substorm number R_{ss} is included in both panels (green curve, right y-axis). Declining phases of SC22 and SC23, dSC23, are marked by dotted vertical lines.

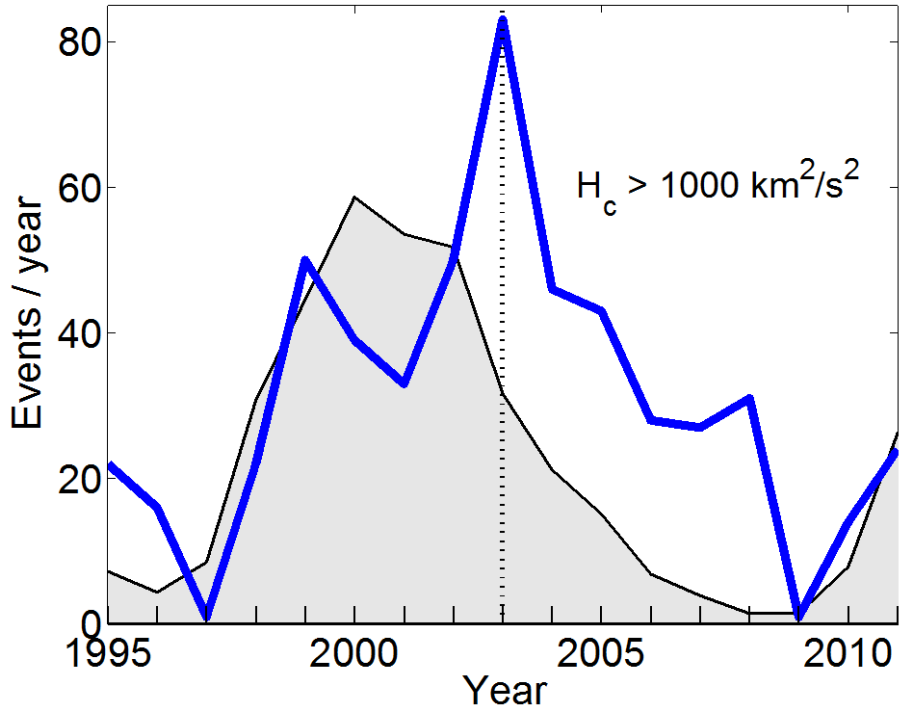

Figure 5. Yearly number of ALFs with cross helicity H_c > 1000 km^2/s^2 (blue line). Sunspot numbers are shown as a gray shaded area for reference. Year 2003 is marked by a dotted vertical line.

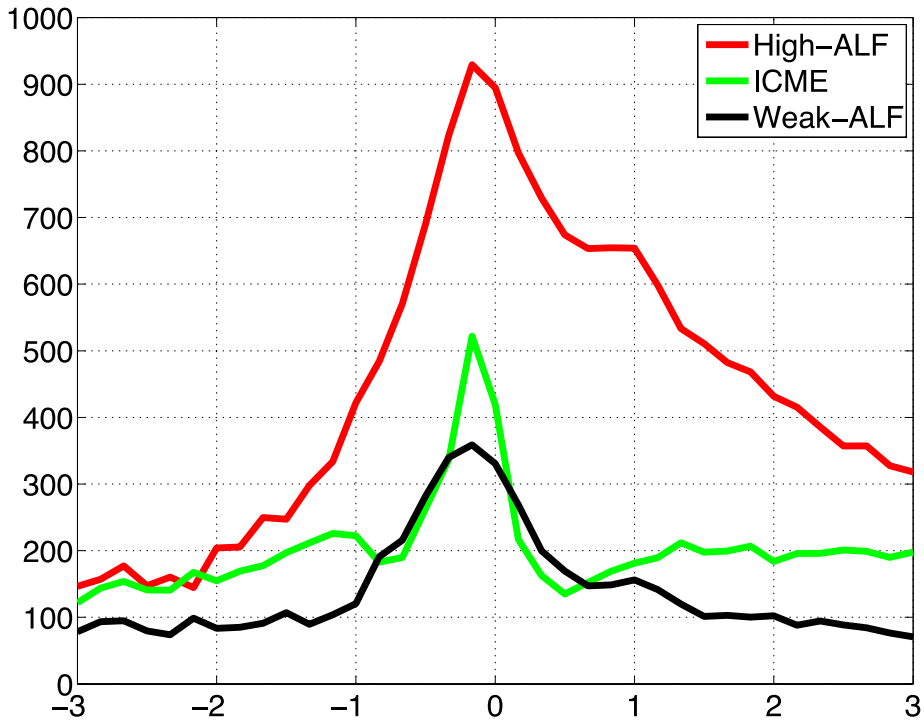

Figure 6. Superimposed epoch plot of cross helicity for high-ALF (red curve), ICMEs (green curve) and weak-ALFs (black curve) from three days before to three days after the zero epoch time (maximum solar wind speed).

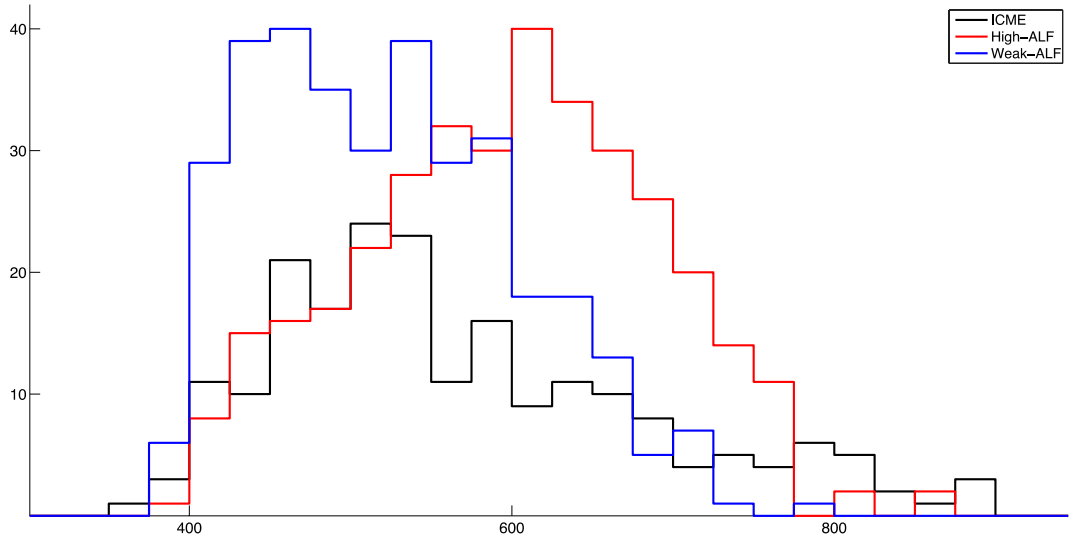

Figure 7. Distribution of solar wind speed during highly Alfvénic solar wind streams (high-ALF), weakly Alfvénic solar wind streams (weak-ALF) and interplanetary coronal mass ejections (ICME).

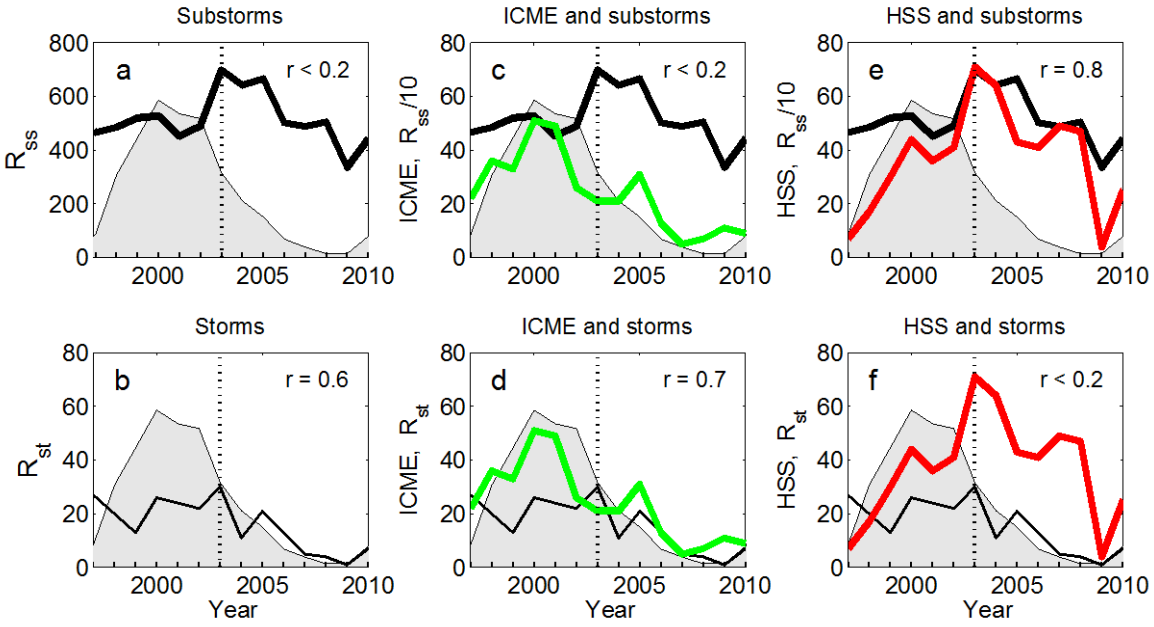

Figure 8. Yearly averaged numbers of geomagnetic storms and substorms and their main drivers (ICMEs and HSSs). Yearly averaged sunspot number (gray shaded area) are included in all panels for reference. (a) Yearly substorm number R_{ss} (thick black curve); (b) Yearly storm number R_{st} (thin black curve); (c) R_{ss} and yearly occurrence of ICMEs (green curve); (d) R_{st} and yearly occurrence of ICMEs (green curve); (e) R_{ss} and yearly occurrence of HSSs (red curve); (f) R_{st} and yearly occurrence of HSSs (red curve). Linear correlation coefficients r between the two lines (c - f) or sunspots and the line (a - b) are shown in the upper right corner of each panel. Year 2003 is marked by a dotted vertical line in each panel.